

CHAPTER 2

Oxidative dissociation of p53 is dependent upon response element DNA

Adapted from Schaefer, K. N. and Barton, J. K. (2014) *Biochemistry* 53, 3467–3475.

INTRODUCTION

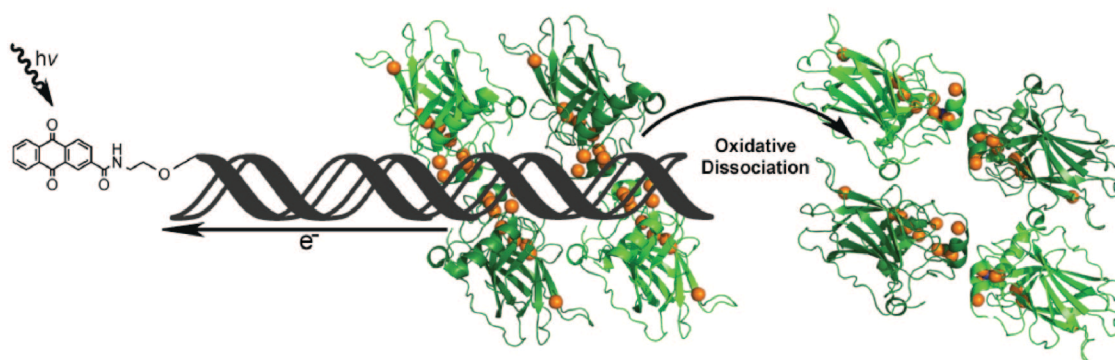
Human transcription factor p53 is warmly referred to as the guardian of the genome, since it plays a critical role in sensing cellular stress and appropriating an according response. Thus far, nearly 150 genes have been identified and validated as being under the direct regulation of this transcription factor.^{1,2} For a gene to be regulated by p53 it must contain a p53 response element within the upstream regulatory region of the gene under regulatory control, typically several hundred base pairs 5' of the transcriptional start site.^{1,2} When p53 binds to a given response element, depending on the gene in question, gene expression may either be activated or repressed; however, a recent computational analysis suggests that p53 is solely a gene activator.^{2,3} It is through N-terminal phosphorylation of cytoplasmic p53 that it is activated, causing it to be transported to the nucleus, and function as a transcription factor.⁴ Much research on p53 has focused on determining its transcriptional targets and untangling the intricate interplay of the protein signaling networks in which it is involved. Although much work has been done to elucidate how p53 actively regulates genes, much still needs to be learned about how p53 selectively chooses which genes to promote and how these corresponding signals are again turned off at the according time.

As a transcription factor, human p53 is known to bind to specific genomic locations to regulate expression of certain genes. The p53 response element was experimentally determined through immunoprecipitation and genetic mapping of DNA fragments bound to p53.⁵ From the cumulative results of 18 distinct binding sites, the p53 response element was determined. The DNA sequence to which p53 was found to recognize and bind is composed of two copies of the 10 base pair half site motif

5'-RRRCWWGYYY-3', separated by 0-13 base pairs, with R representing a purine, Y representing a pyrimidine, and W being either an adenine or a thymine.⁵ Each half site of the p53 response element has striking internal symmetry, and the entire response element is composed of four 5'-RRRCW-3' quarter sites of alternating direction.⁵ The determined p53 response element was consistent with *in vivo* and *in vitro* studies of the time, suggesting that p53 is able to assemble into a homotetramer.^{6,7} Structural analysis via crystallography has also confirmed that p53 self assembles as a tetramer on response element DNA, with each monomer of the p53 tetramer occupying an individual 5'-RRRCW-3' quarter site.⁸ Interestingly, the construct of this response elements allows for hundreds of different distinct DNA sequences simultaneously conforming to this pattern. The determination of the p53 response element led to an explosion of research seeking to determine the genes which p53 regulates as a transcription factor and the physiological impact cellular activity.

In response to DNA-mediated oxidation, p53 bound to its response element DNA has been observed to relinquish its binding to DNA. Investigations of the oxidative dissociation of p53 via DNA charge transport (CT) has led to the study of several synthetic and natural p53 response elements *in vitro*. Oligonucleotide constructs were therefore designed to contain a p53 response element, flanked 5' end with a 12 base pair linker, to which an anthraquinone (AQ) photooxidant is covalently appended.⁹ Excitation of AQ via irradiation abstracts an electron from the DNA, leaving an electron hole among the bases.^{10,11} The electron hole then equilibrates along the π -stacked helical axis and is able to oxidize DNA-bound p53, which leads to its dissociation, as depicted in Figure 2.1. It has been found that the oxidative dissociation of p53 in this system is

FIGURE 2.1 — DNA-mediated oxidation of p53 *in vitro*. Schematic illustration of DNA-mediated CT to promote oxidation and dissociation of DNA-bound p53 (green). Distally tethered to oligonucleotide, AQ serves as the photooxidant to selectively oxidize DNA. Upon photoexcitation, the AQ abstracts an electron from the DNA, leaving an electron hole in the DNA duplex that can equilibrate through the DNA to p53, resulting in protein oxidation. The DNA-mediated oxidation of p53 induces a change of p53, resulting in its dissociation, potentially through a conformational change by disulfide formation within the protein.



indeed DNA-mediated, since the insertion of a DNA mismatch between the AQ and the p53 response element ablates p53 dissociation.⁹ Two human p53 response elements were also studied using the aforementioned construct. The first human p53 response element investigated was cyclin-dependent kinase inhibitor p21 (p21), which is activated by p53 binding and is known to block cell cycle progression out of G1.¹² The second human p53 response element investigated was Gadd45, which is also activated by p53 and is involved in the repair of DNA damage.¹² Apart from being undoubtedly controlled by p53, these two response elements were ideal to study, since they contain the same overall GC% and both sequences for p21 and Gadd45 fully conform to the response element constraints.^{5,12} The binding affinities of reduced p53 are also comparable for both p21 and Gadd45, as determined through electrophoretic mobility shift assays (EMSA).⁹ DNA-mediated oxidative dissociation of p53 as studied by EMSA determined that p53 readily dissociates from the Gadd45 response element but remains bound to the p21 response element under the same experimental conditions.⁹

The only difference between these two response elements is the order in which the DNA bases are arranged, urging that the DNA sequence of the response elements exert a level of control over p53 in its response to oxidative DNA CT. Interestingly, this sequence selectivity with regard to p53 dissociation as observed *in vitro* appears to correlate with sensical biological regulation of p53 under conditions of severe oxidative genomic stress. Since Gadd45 is involved in DNA repair, dissociation of p53 in response to severe genomic oxidation will lead to an overall downregulation, causing the cell to relinquish futile repair processes.⁹ Concurrently, p21 promotes G1 cell cycle arrest, and

continued activation by p53 under severe oxidative genomic stress may lead to cellular senescence and possibly apoptosis.⁹

Due to the contrasting p53 responses from the Gadd45 and p21 response elements, we set out to determine how the p53 response element can dictate whether or not DNA-bound p53 will respond to DNA-mediated oxidation. Our goal is to understand the basis for the DNA sequence selectivity associated with the oxidative dissociation of p53. To investigate this property, we constructed a variety of synthetic response element constructs to tune the one-electron oxidation potentials within the response element, while simultaneously conforming to the response element constraints. Since guanine has the lowest one-electron oxidation potential of all the bases, it serves as an efficient electron hole trap and reactivity correspondingly increases for a guanine doublets and triples, a known hallmark of one-electron DNA oxidation.^{13,14} Once the oxidative dissociation of p53 in response to DNA CT was determined on the synthetic response elements, naturally occurring human response elements were then investigated in the same manner. From the information learned herein, we were able to explore how the sequence context may play a role in p53 regulation more generally, enabling us to make predications about the response of p53 to oxidative DNA CT bound to other human response elements.

MATERIALS AND METHODS

Oligonucleotide synthesis and purification. Oligonucleotides were synthesized on an ABI 3400 DNA synthesizer using standard solid phase phosphoramidite chemistry. Light control sequences (LC) not containing a photooxidant were synthesized with the

dimethoxytrityl (DMT) group intact. Cleavage of the oligonucleotide from the resin and deprotection were conducted by incubation in NH_4OH overnight at 60 °C, and subsequently dried *in vacuo*. The oligonucleotides were purified by reversed phase C-18 HPLC (2% to 32% acetonitrile against 50 mM ammonium acetate over 30 min) with the main peak collected and dried *in vacuo*. DMT removal was conducted by a 15 min incubation of the sample solvated in 80% acetic acid. This reaction was then quenched by the addition of 200 proof ethanol and 3 M sodium acetate. Once dry, the oligonucleotides were subjected to reversed phase HPLC once more (2% to 17% acetonitrile against 50 mM NH_4OAc over 30 min).

Oligonucleotides for the anthraquinone (AQ) photooxidant tethered stands were synthesized with the DMT group removed. An AQ derivative, carboxylic acid(2-hydroxyethyl)amide was converted to its respective phosphoramidite and incorporated onto the 5' end of the sequence using a 15 min coupling on the ABI 3400 DNA synthesizer.⁹⁻¹¹ AQ-conjugated oligonucleotides were cleaved from the resin and deprotected as previously described. The AQ-DNA was purified by reversed phase HPLC (2% to 17% acetonitrile against 50 mM NH_4OAc over 30 min), collecting the peak with absorbance for both DNA at 260 nm and AQ at 365 nm. Oligonucleotides were column desalted (Sep-pak, Millipore), characterized by MALDI-TOF mass spectrometry (Applied Biosystems Voyager DE-PRO), and quantified by UV-visible spectroscopy (Beckman DU7400 spectrophotometer) at their respective ϵ_{260} values. Double stranded oligonucleotides were formed by thermal annealing of equimolar amounts of complementary single strand, heating at 90 °C for 5 min and cooling to ambient temperature in 5 mM sodium phosphate, 50 mM NaCl, pH 7.5.

Protein production. The p53' protein used is a full-length human p53 containing three stabilizing mutations: M133L, V203A, and N268D.¹⁵ The gene for p53' was cloned from the quadruple mutant p53 plasmid N239Y/M133L/V203A/N268D.¹⁵ PCR mutagenesis by overlap extension and gene splicing was used to restore N239 and the sequence was verified by Laragen.¹⁶ The plasmids were propagated in DH5 α cells grown on 2yt media (16 g tryptone, 10 g yeast extract, 5 g NaCl; per 1L) plates with 30 μ g/ml kanamycin plates and isolated using a miniprep kit (Qiagen). The p53' protein was overexpressed and purified as described previously.¹⁷ The protein was overexpressed in BL21(DE3) cells 2yt media with kanamycin and grown at 37 °C to a volume of 6 L and an optical density at 600 nm of 0.6-0.8. The cells were induced by 1mM of IPTG and 0.1 mM of zinc sulphate and allowed to express for 16 hours at 22 °C. At this point the cells should be pelleted by centrifugation and frozen at -80 °C.

The cells then can be defrosted on ice and suspended in nickel column buffer (50 mM KPi, pH 8; 300 mM NaCl; 10mM imidazole; 15 mM β -mercapto-ethanol and one complete protease inhibitor 1 tablet per liter) and manually homogenized. The homogenized cells were then lysed via microfluidization. The lysate was then cleared by centrifugation and filtered through a 0.2 micron sterile filter unit. The protein was first purified by FPLC using a heparin column, using a linear gradient over 10 column volumes to a final concentration of nickel column elution buffer (50 mM KPi, pH 8; 500 mM NaCl; 10mM imidazole; 15 mM β -mercapto-ethanol and one complete protease inhibitor 1 tablet per liter). The isolated protein was digested overnight at 4 °C with TEV protease (Invitrogen) overnight to remove the appended His tag. The protein isolate was then purified once more using FPLC with a heparin column, from 25 mM phosphate, pH

7.5, and 10% glycerol to 25 mM phosphate, pH 7.5, 1.0 M NaCl, and 10% glycerol over 10 column volumes. Dithiothreitol was diluted to nanomolar levels with p53 buffer (20 mM Tris, 100 mM KCl, 0.2 mM EDTA, 20% glycerol, pH 8.0) before the protein was flash-frozen and stored at -80 °C.

5' oligonucleotide radiolabeling. Single stranded oligonucleotides were 5' labeled with ^{32}P -g-dATP (Perkin Elmer) as described.¹⁸ Purification of the oligos via denaturing gel electrophoresis is essential prior to annealing. The purified samples were dried *in vacuo* and resuspended in 5 mM potassium phosphate, 50 mM NaCl, pH 7.5.

3' oligonucleotide radiolabeling. 3' radiolabeling was carried out for DNA strands conjugated with anthraquinone at the 5' end. The AQ oligonucleotides were radiolabeled using ^{32}P - γ dTTP (MP Biomedicals) and Terminal Transferase (New England Biolabs). The samples were mixed at standard NEB protocol conditions, incubated for 2 h at 37 °C, and subsequently passed through two Micro Bio-Spin 6 columns at 3,000 RPM. Purification of the oligos via denaturing gel electrophoresis is essential prior to annealing, and does not affect the tethered AQ. Samples were purified as previously described and the dried purified samples were resuspended in 5 mM potassium phosphate, 50 mM NaCl, pH 7.5.¹⁸

Electrophoretic mobility assay of p53'. The p53' protein was allowed to bind to the radiolabeled oligonucleotides with a 1:1 DNA:protein tetramer ratio (100 nM 1% 5' radiolabeled duplex and 400 nM p53 monomer) in the presence of 5 μM competitor DNA (5'GGAAAAAAAAAAAAAAAAAAACC-3')(IDT), 0.1% NP-40 (Surfact-Amps NP-40, Thermo Scientific), and 0.1 mg/ml BSA (Fraction V, Sigma) in 20 mM Tris-HCl, pH 8.0, 20% glycerol, 100 mM KCl, and 0.2 mM EDTA. The concentration of p53' used

was dependent upon the K_D of the protein for the natural response elements, ensuring a minimum of 80% DNA bound with p53. Samples were made at 4 °C and irradiated on ice for varying lengths of time using a solar simulator (ORIEL Instruments) with a 1000 W Me/Xe lamp, and internal and external UVB/UVC longpass filters to avoid direct DNA strand damage. The radioactivity of each sample was determined by scintillation counting (Beckman LS 5000TD) and normalized prior to loading onto a 10% TBE polyacrylamide gel (Bio-Rad), with the ideal intensity of 300,000 c.p.m. per hour of irradiation of each sample. Each gel was run in 0.5x TBE buffer at 4 °C and 50 V for 1.5 h. DNA from the gel was transferred to Amersham Hybond-N nucleotide blotting paper (GE Healthcare) by semi-dry electroblotter (Owl HEP-1) for 1 h at 175 mA in transfer buffer (25 mM Tris, HCl, 200 mM glycine, 10% methanol, pH 8.5). The blots were exposed to a blanked phosphorimaging screen (GE Healthcare), imaged by a STORM 820 scanning system (Molecular Dynamics), and analyzed using Image Quant, Excel, and Origin. All data were normalized to the corresponding unirradiated control, and the change in p53 binding was determined by monitoring the signal of free DNA over the total DNA signal per lane.

Assay of oxidative DNA damage. Samples were prepared from a stock solution containing 1 μ M 100% 32 P-3' labeled oligomer duplex on the AQ strand, 5 μ M competitor DNA, 0.1% NP-40, and 0.1 mg/mL BSA in p53 buffer (20 mM Tris HCl, 100 mM KCl, 0.2 mM EDTA, 20% glycerol, pH 8.0), with the titration of p53' ranging from 0 to 40 μ M. DNA damage was induced by sample irradiation for 1 h while in an ice-water bath, using a solar simulator with internal and external UVB/UVC longpass filters. Irradiated samples were subsequently treated with a 10% piperidine (Sigma) solution

with 0.2 units of calf thymus DNA in water, and heated at 90 °C for 30 min to cleave damage sites. Piperidine was removed by drying samples *in vacuo*, suspending again in water, and drying *in vacuo* once more. The DNA was ethanol precipitated to ensure purity, although in retrospect this step caused the loss of our lower molecular weight DNA pieces. Scintillation counting was used to ensure that equivalent levels of radioactivity were used in each lane. The dry samples were resuspended in denaturing formamide loading buffer, heated for 2 min at 90 °C, then loaded per lane onto a pre-run 20% polyacrylamide gel and run at 90 watts for 3 h in 1x TBE buffer. Sequencing lanes were created by standard Maxam-Gilbert Sequencing reactions.¹⁹ Gels were visualized by phosphorimagery and quantified using ImageQuant TL and Excel.

RESULTS

p53'-DNA electromobility gel shift assays with synthetic p53 response elements.

The protein used in all of the following experiments is a full-length human p53 containing three thermodynamically stabilizing mutations: M133L, V203A, and N268D.¹⁵ This mutant protein is designated as p53'. The stabilizing mutations for p53' were based on research from the Fersht laboratory for a stabilized yet active p53.¹⁵ For the three mutations in use, preliminary experiments determined that p53' maintained its capacity to respond to oxidative DNA CT by dissociation. Four synthetic DNA response elements were constructed and used for *in vitro* experiments to determine the influence of the guanine pattern in enabling oxidative dissociation of DNA-bound p53' by DNA CT. The oligonucleotides were designed to contain the canonical p53 response element pattern comprised of two response element half sites with no linking bases between the

sites. As seen in Figure 2.2, the response element site is flanked 5' with a 12 base pair linker to which the anthraquinone photooxidant (AQ) is covalently appended, and a ^{32}P radiolabel for the visualization of the DNA is located on the 5' end of the complementary strand. DNA-mediated oxidation of p53' induces a change in protein affinity for response element DNA and promotes its dissociation, which we can monitor by EMSA.

The purine content of the four synthetic constructs range from containing no sequential guanine bases to four sets of guanine triplets, all while fully conforming to response element constraints. Relative reactivity of the bases to one-electron oxidation varies as follows: 5'-GGG > 5'-GG > 5'-GA > 5'-AA.^{13,14} Dissociation constants for p53' to these oligonucleotides lacking AQ are provided in Table 2.1. The change in p53' binding upon photooxidation is determined as the fraction of free DNA signal over total DNA signal per lane, normalized to its respective un-irradiated control, with error bars reflecting the standard error of the mean obtained over a minimum of three replicates. All samples contained 100 nM of response element DNA and 400 nM of p53' to ensure a 1:1 ratio of DNA to p53' tetramer.

The degree of p53' oxidative dissociation is found to vary according to the sequence of the oligonucleotide and is dependent upon photoexcited anthraquinone, as depicted in Figure 2.3. All constructs of light control DNA strands (LC), which are irradiated but do not contain an appended anthraquinone for oxidation, display negligible dissociation of p53'. Dissociation from all of the sequences displays a relatively linear trend with respect to irradiation time, with a maximum dissociation of p53' observed after 30 min. Longer irradiation past 30 min did not significantly increase overall p53

FIGURE 2.2 — Oxidative dissociation of p53' by EMSA from sequences with varied redox potentials. Top: The oligonucleotide construct for investigating the DNA-mediated oxidation of p53' contains the p53 response element. Oxidative DNA CT is induced by irradiation of the appended anthraquinone photooxidant. The red asterisk of the complementary strand denotes the location of the ^{32}P label for visualization. Bottom: Representative autoradiogram of a p53' EMSA of the synthetic GGG sequence. Light control samples do not have an anthraquinone photooxidant conjugated to the DNA, and the overall amount of DNA-bound p53' changes minimally with irradiation. The anthraquinone samples contain the appended AQ photooxidant, and an increase in the amount of lower-molecular weight free DNA is observed with respect to irradiation time.

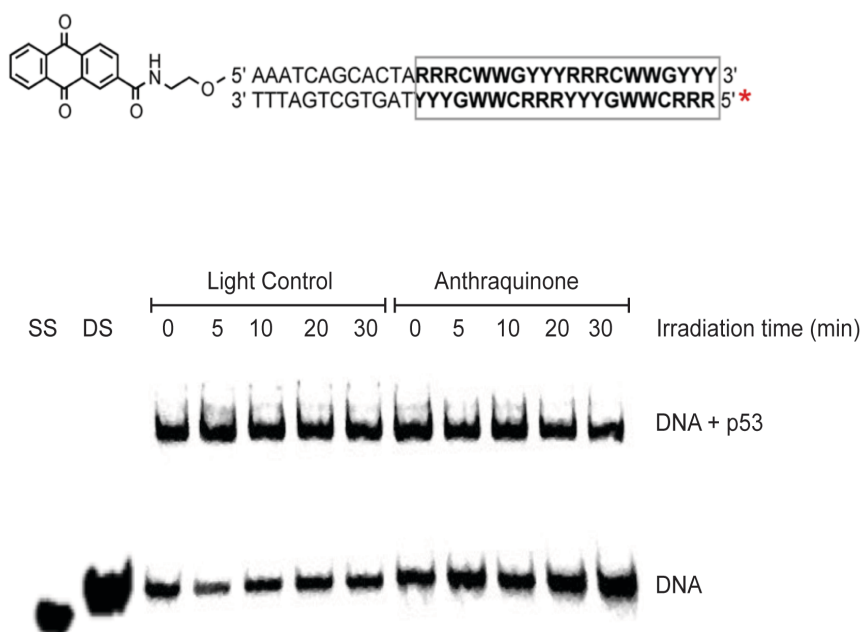


TABLE 2.1 — Oligonucleotide constructs for synthetic and natural p53 response elements studied by EMSA.

Construct Name	DNA Sequence (5'-3') ^a	K _D (nM) ^b	GC % ^c	GG ^d	GGG ^e
AAA	AAATCAGCACTA <u>AAA</u> CATGTCT <u>AAA</u> CATGTCT	230 ± 40	30.0 %	-	-
AGG	AAATCAGCACTA <u>AGG</u> CATGTCT <u>AGG</u> CATGTCT	430 ± 110	50.0 %	2	-
GGG	AAATCAGCACTA <u>GGG</u> CATGTCT <u>GGG</u> CATGTCT	360 ± 70	60.0 %	-	2
GGG/GGG	AAATCAGCACTA <u>GGG</u> CATG <u>CCCCGGG</u> CATG <u>CCC</u>	220 ± 40	80.0 %	-	4
CASP1	AAATCAGCACTAATA <u>AAAG</u> CATGCAT <u>ATG</u> CATGCACA	610 ± 80	36.0 %	-	-
S100A2	AAATCAGCACTA <u>GGG</u> CATGTGT <u>GGG</u> CACGTTTC	330 ± 20	65.0 %	-	2

a. Locations of altered purine nucleobases in direct p53 contact are underlined in the synthetic constructs.

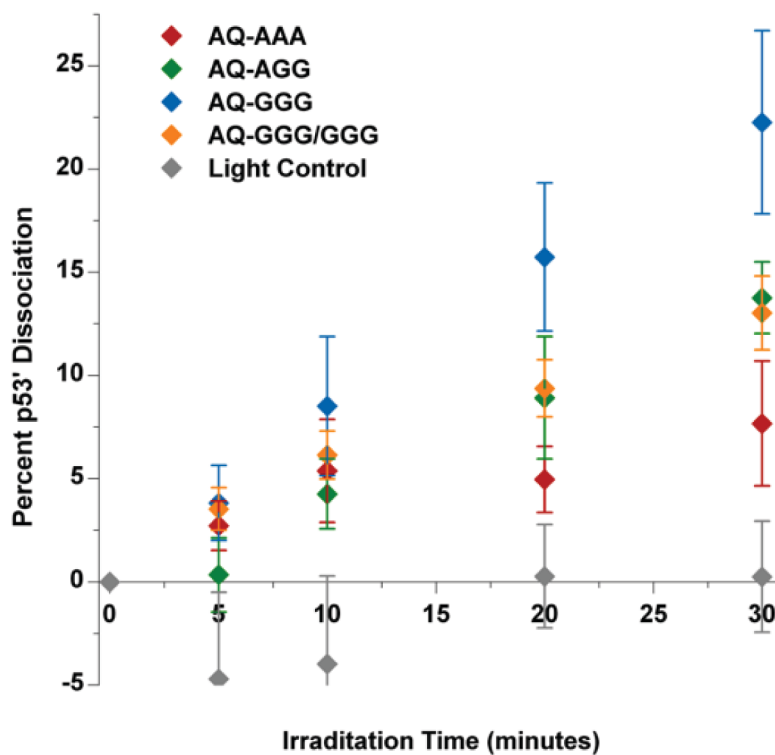
b. Apparent K_D of p53' was determined at 100 nM duplex, 5 μM dAdT, 0.1% NP-40, 0.1 mg/ml BSA in 20 mM TrisCl (pH 8.0), 20% glycerol, 100 mM KCl, and 0.2 mM EDTA and electrophoresed at 4 °C and 50 V on a 10% polyacrylamide gel in 0.5x TBE.

c. GC% of response element, not including 5' linker.

d. Number of guanine doublets within the response element.

e. Number of guanine triplets within the response element.

FIGURE 2.3 — Oxidative dissociation of p53' from synthetic p53 response elements. A plot quantifying the percent change in p53'-DNA binding with respect to irradiation time for the four different synthetic response elements compared to the LC. Sequence constructs are located in Table 2.1. The percent change in p53' binding is determined as the free DNA signal over the total lane signal, normalized to the unirradiated control. Error bars reflect the standard error of the mean over a minimum of three replicates. Samples contained 100 nM duplex, 400 nM p53' monomer, 5 μ M dAdT, 0.1% NP-40, 0.1 mg/ml BSA in 20 mM TrisCl (pH 8.0), 20% glycerol, 100 mM KCl, and 0.2 mM EDTA.



oxidative dissociation. The AQ-AAA sequence confers the least amount of oxidatively induced dissociation of p53' with a maximum dissociation of 7.7%. The AQ-AGG and AQ GGG/GGG sequence both display similar extents of dissociation with a maximum of 13.8% and 13.0%, respectively. The DNA sequence that displayed the greatest amount of p53' dissociation is AQ-GGG at 22.3%. Thus the highest levels of DNA CT oxidative dissociation of p53' were observed from response elements with low redox potential guanine doublets and triplets.

p53'-DNA electromobility shift assays with human p53 response elements.

To determine whether the gel shift results obtained from the synthetic sequences are applicable to naturally occurring human p53 response elements, two human p53 response elements were also investigated: Caspase1A (CASP) and S100 calcium binding protein A2 (S100A2). DNA sequence constructs using their respective response elements and their relative dissociation constants are also shown in Table 2.1. Caspase1A is a cysteine-dependent aspartate-directed proteases and plays essential roles in apoptosis, necrosis, and inflammation.²⁰ This human p53 response element promotes the production of caspase when p53 is bound. The response element of Caspase1A is similar to the synthetic AAA sequence, with an adenine triplet within the purine region of the response element and no guanine doublets or triplets in either of the complementary strands.²⁰ Conversely, the S100A2 protein is intimately involved in cell cycle progression, cellular differentiation, and may function as a tumor suppressor.^{21,22} When p53 is bound to this guanine-rich sequence, S100A2 protein production is promoted. The S100A2 response element is very similar to the synthetic GGG sequence, containing two guanine triplets

within the purine regions. The human response elements were constructed in the same manner as the synthetic sequences above, with an appended 5'-anthraquinone photooxidant, the same 12 base linker, and the complementary strand labeled with 5' ^{32}P -ATP. The relative dissociation constant (K_D) for p53 with each sequence was determined by gel shift assay and quantified by ImageQuant and Excel, and located in Table 2.1.

Experiments were conducted at the protein concentration at which 80% of the radiolabeled oligonucleotides were bound with p53', based upon their respective K_D values (500 nM for the S100A2 sequence and 800 nM for the Caspase1 sequence). As seen in Figure 2.3, the AQ-S100A2 sequence with two guanine triplets yields oxidative dissociation of bound p53' at 14.0%, while the AQ-Caspase1 sequence yields significantly less oxidative dissociation, with a maximum of 6.4%. These sequences do not oxidize p53 linearly with irradiation, instead leveling out at earlier irradiation time points.

Comparison between natural and synthetic p53 response elements.

Figure 2.5 shows the direct comparison between synthetic and natural human sequences. We find that synthetic and natural response elements with varied oxidation potentials due to altered purine patterns within the p53 response element exhibit the following trend in increasing p53 oxidation: AQ-AAA, AQ-Caspase1A (red) < AQ-GGA, AQ-GGG/GGG, and AQ-S100A2 (blue) < AQ-GGG (green).

The AQ-Caspase1A sequence displays minimal dissociation of p53' upon photooxidation, comparable to that seen with the synthetic AQ-AAA sequence. The high redox potential adenine triplet within the purine region does not allow for facile transfer of an electron hole from the DNA to the bound p53'. The AQ-S100A2 sequence, in

FIGURE 2.4 — Oxidative dissociation of p53' from human response elements. A plot quantifying the percent change in p53'-DNA binding with respect to irradiation time for the natural human p53 response elements Caspase1A and S100A2. Sequence constructs are located in Table 2.1. The fraction of p53' dissociation was determined as a ratio of the percent of bound DNA in the irradiated sample to that in the dark control. Error bars reflect the standard error of the mean obtained from a minimum of four trials. Samples contained 100 nM duplex, 500 nM p53 monomer for S100A2, and 800 nM for p53 monomer CASP, 5 μ M dAdT, 0.1% NP-40, 0.1 mg/ml BSA in 20 mM TrisCl (pH 8), 20% glycerol, 100 mM KCl, and 0.2 mM EDTA.

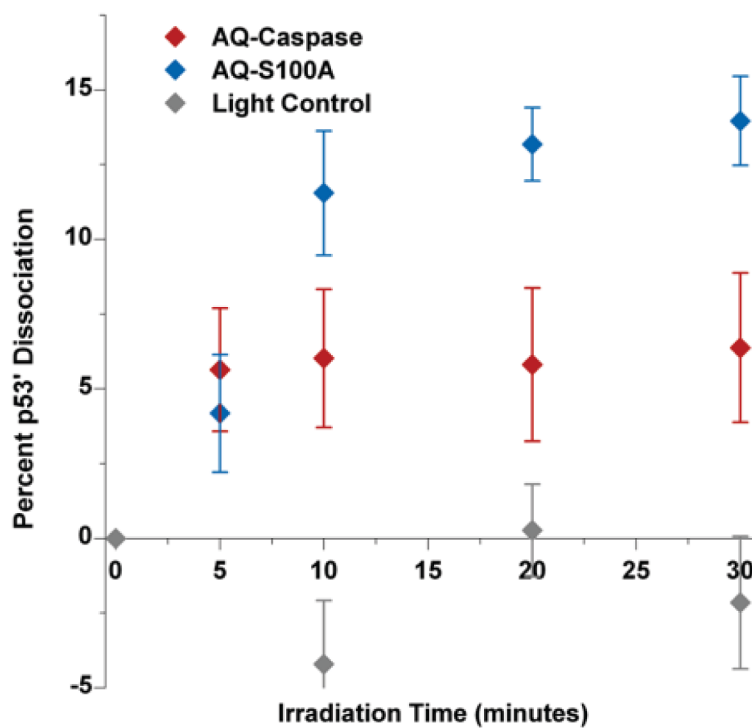
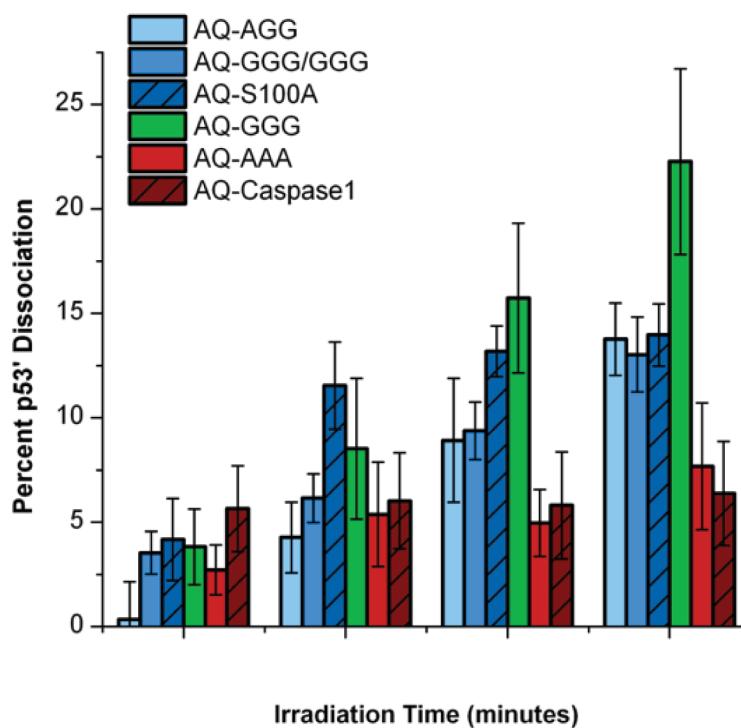


FIGURE 2.5 — Synthetic and human p53 response element EMSA comparison. Comparison of synthetic and natural human p53 response element DNA EMSA data. On the right in red, AQ-CASP1 and AQ-AAA display minimal oxidative dissociation even at long irradiation times. The sequences that allow for oxidative dissociation of p53' (AQ-S100A2, AQ-AGG, and AQ-GGG/GGG) are compared on the left in blue. AQ-GGG in green displays the most oxidative dissociation of p53'.



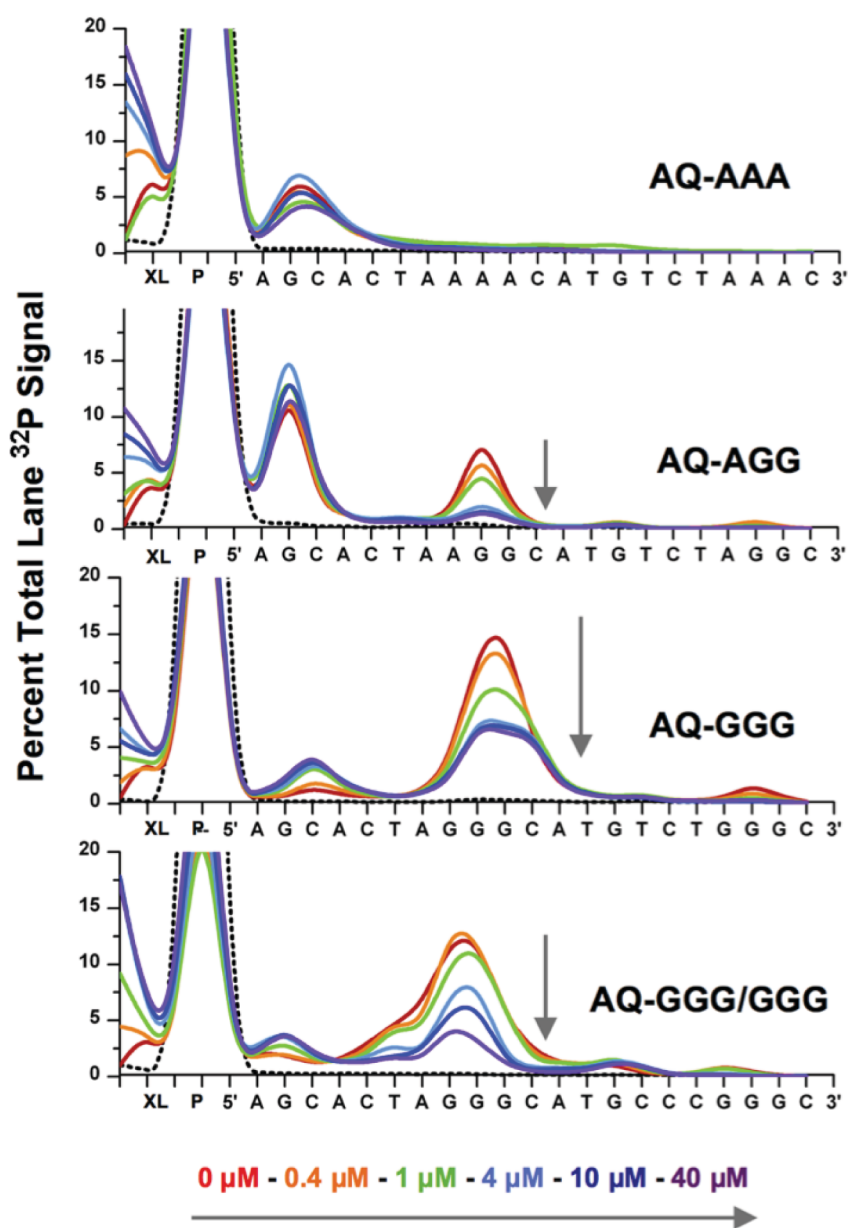
contrast, displays high levels of oxidative dissociation upon irradiation, similar to the AQ-AGG and AQ-GGG/GGG synthetic sequences at 30 minutes of irradiation. Therefore, even with different sequences the guanine pattern within the purine region of the response element allows for equivalent oxidative dissociation of p53' with equivalent amounts of irradiation.

Long range oxidative damage with and without p53' examined by denaturing polyacrylamide gels.

To determine the exact locations within the synthetic oligonucleotides to which the electron holes localize, denaturing polyacrylamide gels were used to determine sites of oxidative DNA damage. The oligonucleotides were 3'-³²P radiolabeled on the AQ strand for visualization, and treated with piperidine to cleave the DNA backbone at the site of oxidative damage.¹⁹ When compared to Maxam-Gilbert sequencing lanes and the un-irradiated control, the locations of DNA oxidative damage induced by photooxidation are observed as bands on the denaturing polyacrylamide gel. The intensity of each piperidine cleavage site is measured in comparison to the total signal intensity of each lane. The p53' protein was also titrated into the samples to assess how the protein inhibits DNA damage. The presence of p53' inhibits DNA damage by transfer of the electron hole from the DNA to the protein, as shown in Figure 2.6 and Figure 2.7.

Oxidative damage is apparent primarily at the 5'-G of guanine doublets and triplets within the response elements, as expected thermodynamically. After an hour of irradiation for the AQ-AAA sequence, which lacks guanine repeats, oxidative damage is observed only at the single 5'-G located near the tethered oxidant; this guanine is not contained within the response element. Additionally, damage at this guanine is not

FIGURE 2.6 — Representative guanine oxidation gel shift assay analysis. The four 3' radiolabeled synthetic response element lane profiles are displayed at varying protein concentrations. The gels were analyzed using Imagequant, and each band was calculated as the percent of total lane signal. The dotted black line represents the unirradiated control. The concentration of p53' in the irradiated samples is varied from 0 μM (red) to 40 μM (purple) p53' monomer. Samples contained 1 μM AQ-Duplex, 5 μM dAdT, 0.1% NP-40, 0.1 mg/ml BSA in 20 mM TrisCl (pH 8), 20% glycerol, 100 mM KCl, and 0.2 mM EDTA.



inhibited upon addition of p53' at any concentration. The AQ-AGG sequence displays damage within the response element primarily at the 5'-GG location and at the single guanine located in the linker region, adjacent to the oxidant. Upon the addition of 10-fold excess p53' tetramer, a full recovery of the damage within the response element guanine doublet is observed. In contrast, no recovery is observed at the single guanine in the linker region. Sequences AQ-GGG and AQ-GGG/GGG both displayed the majority of their oxidatively induced damage at the 5'-guanine triplet site within the response element, with no significant damage in the linker region. The addition of p53' to both AQ-GGG and AQ-GGG/GGG mitigates DNA base damage within the response element. In these sequences the damage is not fully quenched by concentrations of p53' up to 40 μM .

Damage was not readily observed at the purine regions near the 3' end. Ethanol precipitation of the samples may have led to the loss of these low molecular weight products. In all of the sequences, some higher molecular weight products are also observed and can be attributed to the formation of covalently cross-linked products. Irradiation without the addition of p53' gives one band which is indicative of a crosslink between the two DNA strands. The higher molecular weight bands are indicative of possible p53-DNA crosslinks.

DISCUSSION

Sequence dependence of p53' dissociation.

Electron holes in DNA localize to regions of low redox potential, most notably guanine doublets and triplets. Specific sequences of oligonucleotides incorporating

guanine doublets and triplets into the purine regions of the response element site enabled the study of how the guanine pattern in p53 response element binding sites influences oxidative dissociation of p53. Sequences containing low redox potential guanine doublets and triplets enable oxidative dissociation of p53'; we refer to these as responsive sequences. Figure 2.2 shows maximum p53' dissociation from the responsive sequences of AQ-GGG at 22.3%, followed by AQ-AGG, AQ-GGG/GGG around 13.0%. The AQ-AAA sequence confers minimal p53' dissociation of 7.7%, and we categorize this as a non-responsive sequence.

Electron hole occupancy at a particular location can be described in the context of overall residence times. When equilibrating along the π -stacked DNA helical axis, an electron hole will spend more time at a low redox potential GGG site rather than a high redox potential AAA site. The finding that the AQ-GGG/GGG sequence did not yield the most oxidative dissociation of p53' is noteworthy. In the double-stranded promoter site, the AQ-GGG sequence has two locations in which holes can reside, while the AQ-GGG/GGG has four. Effectively, the electron hole density in each GGG site of AQ-GGG/GGG is half of that of AQ-GGG, resulting in approximately half the p53' dissociation as compared to AQ-GGG.

Importantly, the location of low redox potential sites should align with the p53-DNA major groove interface with the p53 DNA-binding domain to enable effective electron transfer. Thus, not all low potential sites within a response element are expected to transfer an electron hole to p53', only those in close contact with the protein. It is known that CT in proteins decays exponentially with distance, highlighting the necessity for low reduction potential bases at the DNA-p53 interface for this process to occur. The

denaturing DNA damage gels of Figure 2.6 and Figure 2.7 illustrate the necessity both of proper p53 contact for electron hole transfer and of the redox potentials of purines in contact with p53 for conferring a sensitive response. As highlighted in the AQ-AAA and AQ-AGG sequences, damage does occur at the guanine in the linker region, but that damage is not inhibited by the addition p53' at any concentration investigated. The inhibition of DNA damage in the presence of p53 is seen only at low redox potential sites in the p53 response element, and therefore in contact with p53'. Moreover, for oxidative dissociation of p53' to occur, the bases in contact with p53' must be able to initially trap the electron hole with an overall low redox potential. Thus the hole localization within the response element ultimately dictates the response the response element will confer for the oxidative dissociation of p53.

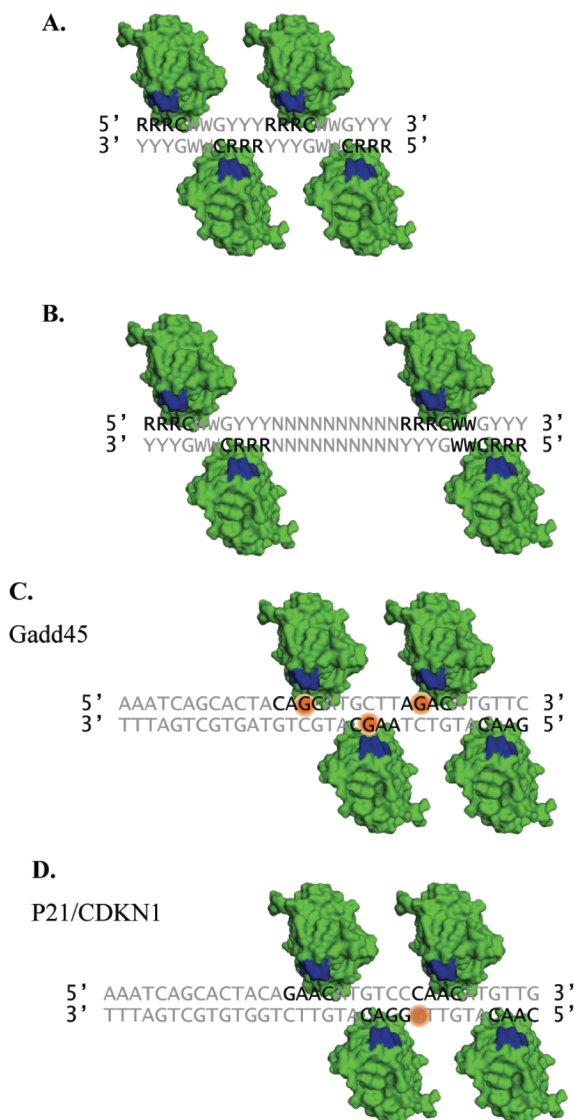
To establish whether natural p53 binding sites respond similarly to the synthetic ones, two sequences were studied. The natural sequences were found to behave similarly to their synthetic counterparts due to similar guanine patterns in the purine region of the response elements. Upon oxidation, p53' dissociates from S100A2, which is similar to the responsive synthetic sequences due to the presence of two guanine triplets; S100A2 is thus classified as a responsive sequence. Since p53 promotes S100A2 expression when bound, oxidative stress would lead to p53 dissociation and subsequent downregulation of the gene, resulting in diminished tumor suppressor activity. In contrast, the CASP1 sequence is similar to the AQ-AAA synthetic sequence. Minimal dissociation of p53' from CASP is observed upon irradiation, designating the CASP p53 response element as non-responsive. Thus, upon oxidation, p53 would be expected to remain mostly bound, leading to the continued promotion of CASP. The continual promotion CASP production

by p53 during times of oxidative genomic stress signals the cell to continue toward apoptosis.

Making predictions about natural p53 response elements under genomic oxidative stress.

We can also compare these results to our earlier work that demonstrated a contrasting oxidation response in p53 between recognition elements corresponding to Gadd45 (DNA repair) and p21 (cell cycle arrest), now known as CDKN1A.⁹ These p53 binding sites contain identical G/C percentages but display different guanine patterns overall. The p53-bound Gadd45 sequence can be classified as responsive, yielding oxidative dissociation of p53. In contrast, little p53 oxidation was seen from the p21 sequence, characterizing this site as non-responsive. Figure 2.8 highlights the p53 residues that nest in the major groove (blue: K120, S121, C277, and R280) and the bases of the response element with which they directly interact (black). As a general example, Figure 2.8A depicts two half-sites with no intervening spacer base pairs, highlighting the importance of low redox potential guanines at the 5'-RRRG-3' site in direct p53 contact for responsiveness. The p53 response element is known to contain a 0-13 base pair linker region between the two p53 half sites; certain p53 binding sites may conform to these designated constraints but contain low redox potential sites that are not in direct contact with p53. Figure 2.8B depicts p53 binding to a response element with a 10 base linker between the two half sites. Guanine triplets located within such a linker region would be favorable locations for electron hole localization, but the electron holes would be funneled away from the direct p53 contact sites and the overall responsiveness of that site

FIGURE 2.8 — Response element DNA–p53 interaction. All diagrams are representations modeled from the 3KMD crystal structure by Chen *et al.*²³ A. p53 tetramer (green) bound to canonical response element represented by letters. The contacting p53 residues are shown in blue and the nucleobases that they hydrogen bond with are noted by black letters. B. Representation of a p53 tetramer bound to a response element with a 10 nucleobase linker between the two half sites C. Representative binding of a p53 tetramer to the Gadd45 response element. The orange circles indicate anticipated locations for an electron hole to localize within direct contact of a p53 monomer. D. Representative binding of a p53 tetramer to the p21 response element. The expected location of electron hole localization is denoted by the orange circle and located between the two half sites and away from direct p53 contact.



would therefore be decreased. The response element sequence for Gadd45 is shown to be responsive by gel shift assay *in vitro*.⁹ Figure 2.8C illustrates that the p53 response element for Gadd45 indeed has guanines directly aligned with the p53 contact residues, and these guanines enable the overall responsiveness of this p53 binding site. The recognition sequence for p21 is shown in Figure 2.8D. This p53 binding site contains a low redox potential guanine triplet in the complement strand, but the 5' guanine is located at the interface of the two half sites, away from the contacting p53 residues in the major groove. Upon oxidation, an electron hole would preferentially localize to the 5' location of the guanine triplet at the interface of the two half sites, out of direct p53 contact, decreasing the opportunity for oxidation of p53, rendering the sequence non-responsive.

These results enable us to make predictions regarding the responsiveness of other human p53 response elements to DNA CT. Out of more than 200 known human p53 binding sites, we focused on sequences containing the canonical 5'-CWWT-3' in both half-sites. An illustrative set of sequences, 21 which we felt confident in making predictions, is provided in Table 2.2.²⁴⁻²⁷ Here, we highlight several interesting p53 response element predictions. Non-responsive p53 binding sites include chromosome 12 open reading frame 5 (C12orf5) and matrix metalloproteinase 2 (MMP2).^{27,28} For both of these genes, p53 serves as an activator. Under conditions of oxidative stress, we predict p53 binding should not be affected by DNA CT and there should be no significant change in the regulation of that gene. C12orf5 will continue to be promoted, directing the glycolysis pathway into the pentose phosphate shunt, while also protecting the cell from reactive oxygen species.²⁷ MMP2, also predicted to be non-responsive, is involved in the

TABLE 2.2 — Predictions of p53 responsiveness to oxidative DNA CT on human response elements.

Gene	First quarter site	Second quarter site	Linker	Third quarter site	Fourth quarter site	Predicted Responsiveness	p53 Activity	Predicted CT Response of p53	Δ gene regulation	Ref.
AIFM2	AGGCA	TGAGC	CACCGTGCCT	GGCCA	AGCCC	AIFM2	Activator	Dissociation	Downregulation	32
	Yes	Yes	Traps	Yes	Yes	Yes				
APAF1	AGACA	TGTCT	GGAGACCCTAGGA	CGACA	AGCCC	APAF1	Activator	Dissociation	Downregulation	33
	No	No	Traps	No	Yes	No				
BBC3	CTGCA	AGTCC		TGACT	TGTCC	BBC3	Activator	Dissociation	Downregulation	34
	Yes	Yes		No	Yes	Yes				
C12orf5	AGACA	TGTCC	AC	AGACT	TGTCT	C12orf5	Activator	Dissociation	Downregulation	35
	No	Yes		No	No	No				
CCNK	AAACT	AGCTT	GC	AGACA	TGCTG	CCNK	Activator	Dissociation	Downregulation	36
	No	Yes		No	Yes	Yes				
CDKN1A	GAACA	TGTCC		CAACA	TGTTG	CDKN1A	Activator	Remains Bound	No Change	37
	No	Yes		No	No	No				
DDB2	GAACA	AGCCC	T	GGGCAT	TGTTT	DDB2	Activator	Dissociation	Downregulation	38
	No	Yes		Yes	No	Yes				
FAS	GGACA	AGCCC		TGACA	AGCCA	FAS	Activator	Dissociation	Downregulation	39
	Yes	Yes		No	Yes	Yes				
GADD45A	GAACA	TGTCT		AAGCAT	TGCTG	GADD45A	Activator	Dissociation	Downregulation	40
	No	No		Yes	Yes	Yes				
IGFBP3	AAACA	AGCCA	C	CAACA	TGCTT	IGFBP3	Repressor	Dissociation	Upregulation	41
	No	Yes		No	Yes	Yes				
MMP2	AGACA	AGCCT		GAACT	TGTCT	MMP2	Activator	Dissociation	Downregulation	42
	No	Yes		No	No	No				
PERP	AGGCA	AGCTC		CAGCT	TGTC	PERP	Activator	Dissociation	Downregulation	43
	Yes	Yes		Yes	No	Yes				
PLK2	AAACA	TGCCT		GGACT	TGCCC	PLK2	Activator	Dissociation	Downregulation	44
	No	Yes		Yes	Yes	Yes				
PPM1J	GAACA	TGCCT		GAGCA	AGCCC	PPM1J	Activator	Dissociation	Downregulation	45
	No	Yes		Yes	Yes	Yes				
PTEN	GAGCA	AGCCC	CAGGCAGCTACT	GGGCA	TGCTC	PTEN	Activator	Dissociation	Downregulation	46
	Yes	Yes (No)	Traps	Yes	Yes	Yes				
RRM2B	TGACA	TGCCC		AGGCA	TGTCT	RRM2B	Activator	Dissociation	Downregulation	47
	No	Yes		Yes	No	Yes				
SCARA3	GGGCA	AGCCC		AGACA	AGTTG	SCARA3	Activator	Dissociation	Downregulation	48
	Yes	Yes		No	No	Yes				
TP63	TAACT	TGTTA	TTG	AAACA	TGCTC	TP63	Activator	Remain Bound	No Change	49
	No	No		No	Yes	No				
TSC2	TAACA	AGCTC	G	GGGCT	AGCCC	TSC2	Activator	Dissociation	Downregulation	50
	No	Yes	Trap	(No) Yes	Yes	Yes				
VCAN	AGACT	TGCCA	C	AGACA	AGTCC	VCAN	Activator	Dissociation	Downregulation	51
	No	Yes		No	Yes	Yes				
VDR	TAACT	AGTTT		GAACA	AGTTG	VDR	Activator	Remains Bound	No Change	52
	No	No		No	No	No				

breakdown of extracellular matrix, which is useful for apoptotic processes.²⁸ In contrast, responsive p53 binding sequences that have been found include damage-specific DNA binding protein 2 (DDB2), polo-like kinase 2 (PLK2), and protein phosphatase, Mg²⁺/Mn²⁺ dependent, 1J (PPM1J).²⁹⁻³¹ In all of these cases, p53 binding promotes the expression of these genes. As these sequences appear to be responsive based on the purine pattern, we predict p53 oxidative dissociation by DNA CT, which will decrease p53 occupancy and cause an overall downregulation of the corresponding gene products. DDB2 is necessary for the repair of DNA damage induced by ultraviolet light within the nucleotide excision repair pathway.²⁹ PLK2 is a member of the polo family of serine/threonine protein kinases, playing a primary role in normal cell division, and is necessary for the G1/S transition.³⁰ PPM1J encodes a serine/threonine protein phosphatase of unknown overall function.³¹ In all of these cases, oxidation should lead to overall gene downregulation, leading to lowered MMR pathway activity and tuning of cell cycle control.

The pattern and location of bases in the p53 binding site have been shown to play a critical role in how p53 may regulate the expression of different genes under conditions of oxidative stress. DNA sequences with triplet guanine sites that make contact with p53 protein binding sites are particularly prone to activate oxidation of the bound protein under conditions of oxidative stress. This protein oxidation offers another layer of regulatory control and a means of modifying specific proteins post-translationally to respond to an environmental signal. The fact that this modification can occur from a distance through DNA CT is more powerful still in permitting a host of regulatory effects on the genome that respond specifically and chemically to the guanine radicals generated

with oxidative stress. Indeed, these results illustrate another unique role to consider for long range CT within the cell.

REFERENCES

1. Miled, C., Pontoglio, M., Garbay, S., Yaniv, M., and Weitzman, J. (2005) A genomic map of p53 binding sites identifies novel p53 targets involved in an apoptotic network. *Cancer Research* 65, 5096-5104.
2. Vousden, K., and Prives, C. (2009) Blinded by the light: The growing complexity of p53. *Cell* 137, 413-441.
3. Fischer, M., Steiner, L., and Engeland, K. (2014) The transcription factor p53: Not a repressor, solely an activator. *Cell Cycle* 13, 3037-3058.
4. O'Keefe, K., Li, H., and Zhang, Y. (2003) Nucleocytoplasmic shuttling of p53 is essential for MDM2-mediated cytoplasmic degradation but not ubiquitination. *Mol. Cell. Biol.* 23, 6396-6405.
5. el-Deiry, W., Kern, S., Pietenpol, J., Kinzler, K., and Vogelstein, B. (1992) Definition of a consensus binding site for p53. *Nat. Genet.* 1, 45-59.
6. Kraiss, S., Quaiser, A., Oren, M., and Montenarh, M. (1988) Oligomerization of oncoprotein p53. *J. Virol.* 62, 4737-4744.
7. Weinberg, R. A. (1991) Tumor suppressor genes. *Science* 254, 1138-1146.
8. Cho, Y., Gorina, S., Jeffrey, P. D., and Pavletich, N. P. (1994) Crystal-structure of a p53 tumor-suppressor DNA complex: Understanding tumorigenic mutations. *Science* 265, 346-354.
9. Augustyn, K., Merino, E., and Barton, J. K. (2007) A role for DNA-mediated charge transport in regulating p53: Oxidation of the DNA-bound protein from a distance. *Proc. Natl. Acad. Sci. U. S. A.* 104, 18907-18912.
10. Armitage, B., Yu, C., Devadoss, C., and Schuster, G. B. (1994) Cationic anthraquinone derivatives as catalytic DNA photonucleases: Mechanisms for DNA damage and quinone recycling. *J. Am. Chem. Soc.* 116, 9847-9859.

11. Gasper, S. M. and Schuster, G. B. (1997) Intramolecular photoinduced electron transfer to anthraquinones linked to duplex DNA: The effect of gaps and traps on long-range radical cation migration. *J. Am. Chem. Soc.* *119*, 12762-12771.
12. el-Deiry, W., Tokino, T., Velculescu, V., Levy, D., Parsons, R., Trent, J., Lin, D., Mercer, W., Kinzler, K., and Vogelstein, B. (1993) WAF1, a potential mediator of p53 tumor suppression. *Cell* *75*, 817-825.
13. Sugiyama, H., and Saito, I. (1996) Theoretical studies of GG-specific photocleavage of DNA via electron transfer: significant lowering of ionization potential and 5' localization of HOMO of stacked GG bases from B-form DNA. *J. Am. Chem. Soc.* *118*, 7063-7068.
14. Saito, I., Nakamura, T., Nakatani, K., Yoshioka, Y., Yamaguchi, K., and Sugiyama, H., (1998) Mapping of the hot spots for DNA damage by one-electron oxidation: Efficacy of GG doublets and GGG triplets as a trap in long-range hole migration. *J. Am. Chem. Soc.* *120*, 12686-12687.
15. Nikolova, P.V., Henckel, J., Lane, D. P., and Fersht, A. R. (1998) Semirational design of active tumor suppressor p53 DNA binding domain with enhanced stability. *Proc. Natl. Acad. Sci. U. S. A.* *95*, 14675-14680.
16. Vallejo, A. N., Pogullis, R. J., and Pease, L. R. (2008) DNA-mediated oxidation of p53. *Cold Spring Harb. Protoc.* 2008.
17. Veprintsev, D. B., Freund, S. M., Andreeva, A., Rutledge, S. E., Tidow, H., Cañadillas, J. M., Blair, C. M., and Fersht, A. R. (2006) Core domain interactions in full-length p53 in solution. *Proc. Natl. Acad. Sci. U. S. A.* *103*, 2115-2119.
18. Zeglis, B. M. and Barton, J. K. (2007) DNA base mismatch detection with bulky rhodium intercalators: synthesis and applications. *Nat. Protoc.* *2*, 357-371.
19. Maxam, A. M., and Gilbert, W. (1977) A new method for sequencing DNA. *Proc. Natl. Acad. Sci. U. S. A.* *74*, 560-564.
20. Gupta, S., Radha, V., Furukawa, Y., and Swarup, G. (2001) Direct transcriptional activation of human caspase-1 by tumor suppressor p53. *J. Biol. Chem.* *276*, 10585-10588.
21. Wicki, R., Franz, C., Scholl, F. A., Heizmann, C. W., and Schäfer, B. W. (1997) Repression of the candidate tumor suppressor gene S100A2 in breast cancer is mediated by site-specific hypermethylation. *Cell Calcium* *22*, 243-254.

22. Cao, L. Y., Yin, Y., Li, H., Jiang, Y., and Zhang, H. F. (2009) Expression and clinical significance of S100A2 and p63 in esophageal carcinoma. *World J. Gastroenterol.* *15*, 4183-4188.
23. Chen, Y., Dey, R., and Chen, L. (2010) Crystal structure of the p53 core domain bound to a full consensus site as a self-assembled tetramer. *Structure* *18*, 246-256.
24. Riley, T., Sontag, E., Chen, P., and Levine, A. (2008) Transcriptional control of human p53-regulated genes. *Nat. Rev. Mol. Cell Biol.* *9*, 402-412.
25. Geer, L. Y., Marchler-Bauer, A., Geer, R. C., Han, L., He, J., He, S., Liu, C., Shi, W., and Bryant, S. H. (2010) The NCBI BioSystems database. *Nucleic Acids Res.* *D492-6*, 137939.
26. Wilson, D., Charoensawan, V., Kummerfeld, S., and Teichmann, S. (2008) DBD—taxonomically broad transcription factor predictions: new content and functionality. *Nucl. Acids Res.* *36*, D88-D92.
27. Madan, E., Gogna, R., Bhatt, M., Pati, U., Kuppusamy, P., and Mahdi, A. (2011) Regulation of glucose metabolism by p53: emerging new roles for the tumor suppressor. *Oncotarget* *2*, 948-957.
28. Werb, Z. (1997) ECM and cell surface proteolysis: regulating cellular ecology. *Cell* *91*, 439-442.
29. Sun, N. K., Kamarajan, P., Huang, H., and Chao, C. (2002) Restoration of UV sensitivity in UV-resistant HeLa cells by antisense-mediated depletion of damaged DNA-binding protein 2 (DDB2). *FEBS letters* *512*, 168-172.
30. Burns, T., Fei, O., Scata, K., Dicker, D., and el-Deiry, W. (2003) Silencing of the novel p53 target gene Snk/Plk2 leads to mitotic catastrophe in Paclitaxel (Taxol)-exposed cells. *Mol. Cell. Biol.* *23*, 5556-5571.
31. Zolnierowicz, S. (2000) Type 2A protein phosphatase, the complex regulator of numerous signaling pathways. *Biochem. Pharmacol.* *60*, 1225-1235.
32. Wu, M., Xu, L. G., Su, T., Tian, Y., Zhai, Z., and Shu, H. B. (2004) AMID is a p53-inducible gene downregulated in tumors. *Oncogene* *23*, 6815-6819.
33. Robles, A., Bemmels, N., Foraker, A., and Harris, C. (2001) APAF-1 is a transcriptional target of p53 in DNA damage-induced apoptosis. *Cancer Res.* *61*, 6660-6664.

34. Nakano, K. and Vousden, K. H. (2001) PUMA, a novel proapoptotic gene, is induced by p53. *Mol. Cell* 7, 683-694.
35. Bensaad, K., Tsuruta, A., Selak, M., Vidal, M., Nakano, K., Bartrons, R., Gottlieb, E., and Vousden, K. (2006) TIGAR, a p53-inducible regulator of glycolysis and apoptosis. *Cell* 126, 107-120.
36. Mori, T., Anazawa, Y., Matsui, K., Fukuda, S., Nakamura, Y., and Arakawa, H. (2002) Identification of the interferon regulatory factor 5 gene (IRF-5) as a direct target for p53. *Neoplasia* 4, 268-274.
37. Saramäki, A., Banwell, C., Campbell, M., and Carlberg, C. (2006) Regulation of the human p21(waf1/cip1) gene promoter via multiple binding sites for p53 and the vitamin D3 receptor. *Nucleic Acids Res.* 34, 543-554.
38. Tan, T. and Chu, G. (2002) p53 binds and activates the xeroderma pigmentosa DDB2 gene in humans but not mice. *Mol. Cell. Biol.* 22, 3247-3254.
39. Müller, M., Wilder, S., Bannasch, D., Israeli, D., Lehlbach, K., Li-Weber, M., Friedman, S., Galle, P., Stremmel, W., Oren, M., and Krammer, P. (1998) p53 activates the CD95 (APO-1/Fas) gene in response to DNA damage by anticancer drugs. *J. Exp. Med.* 188, 2033-2045.
40. Tamura, R., de Vasconcellos, J., Sarkar, D., Libermann, T., Fisher, P., and Zerbini, L. (2012) GADD45 proteins: central players in tumorigenesis. *Curr. Mol. Med.* 12, 634-651.
41. Buckbinder, L., Talbott, R., Velasco-Miguel, S., Takenaka, I., Faha, B., Seizinger, B. R., and Kley, N. (1995) Induction of the growth inhibitor IGF-binding protein 3 by p53. *Nature* 377, 646-649.
42. Bian, J. and Sun, Y. (1997) Transcriptional activation by p53 of the human type IV collagenase (gelatinase A or matrix metalloproteinase 2) promoter. *Mol. Cell. Biol.* 17, 6330-6338.
43. Reczek, E. E., Flores, E. R., Tsay, A. S., Attardi, L. D., and Jacks, T. (2003) Multiple response elements and differential p53 binding control Perp expression during apoptosis. *Mol. Cancer Res.* 1, 1048-1057.
44. Burns, T. F. (2003) Silencing of the novel p53 target gene Snk/Plk2 leads to mitotic catastrophe in Paclitaxel (Taxol)-exposed cells. *Mol. Cell. Biol.* 23, 5556-5571.

45. Shiiio, Y., Yamamoto, T., and Yamaguchi, N. (1992) Negative regulation of Rb expression by the p53 gene product. *Proc. Natl. Acad. Sci. U. S. A.* 89, 5206-5210.
46. Stambolic, V., MacPherson, D., Sas, D., Lin, Y., Snow, B., Jang, Y., Benchimol, S., and Mak, T. W. (2001) Regulation of PTEN transcription by p53. *Mol. Cell* 8, 317-325.
47. Kuo, M. L., Sy, A., Xue, L., Chi, M., Lee, M., Yen, T., Chiang, M.-I., Chang, L., Chu, P., and Yen, Y. (2012) RRM2B suppresses activation of the oxidative stress pathway and is up-regulated by p53 during senescence. *Sci. Rep.* 2, 822.
48. Herzer, K., Falk, C. S., Encke, J., Eichhorst, S. T., Ulsenheimer, A., Seliger, B., and Krammer, P. H. (2003) Upregulation of major histocompatibility complex class I on liver cells by hepatitis C virus core protein via p53 and TAP1 impairs natural killer cell cytotoxicity. *J. Virol.* 77, 8299-8309.
49. Harnes, D. C., Bresnick, E., Lubin, E. A., Watson, J. K., Heim, K. E., Curtin, J. C., Suskind, A. M., Lamb, J., and DiRenzo, J. (2003) Positive and negative regulation of Δ N-p63 promoter activity by p53 and Δ N-p63- α contributes to differential regulation of p53 target genes. *Oncogene* 22, 7607-7616.
50. Feng, Z., Hu, W., de Stanchina, E., Teresky, A. K., Jin, S., Lowe, S., and Levine A. J. (2007) The regulation of AMPK β 1, TSC2, and PTEN expression by p53: Stress, cell and tissue specificity, and the role of these gene products in modulating the IGF-1-AKT-mTOR pathways. *Cancer Res.* 67, 3043-3053.
51. Yoon, H., Liyanarachchi, S., Wright, F. A., Davuluri, R., Lockman, J. C., de la Chapelle, A., and Pellegata, N. S. (2002) Gene expression profiling of isogenic cells with different TP53 gene dosage reveals numerous genes that are affected by TP53 dosage and identifies CSPG2 as a direct target of p53. *Proc. Natl. Acad. Sci. U. S. A.* 99, 15632-15637.
52. Maruyama, R., Aoki, F., Toyota, M., Sasaki, Y., Akashi, H., Mita, H., Suzuki, H., Akino, K., Ohe-Toyota, M., Maruyama, Y., Tatsumi, H., Imai, K., Shinomura, Y., and Tokino, T. (2006) Comparative genome analysis identifies the vitamin D receptor gene as a direct target of p53-mediated transcriptional activation. *Cancer Res.* 66, 4574-4583.